2013

Transparent, flexible, and solid-state supercapacitors based on graphene electrodes

Y. Gao
University of Nebraska - Lincoln

Y. S. Zhou
University of Nebraska - Lincoln

W. Xiong
University of Nebraska - Lincoln

L. J. Jiang
University of Nebraska - Lincoln

M. Mahjouri-samani
University of Nebraska - Lincoln

See next page for additional authors

Transparent, flexible, and solid-state supercapacitors based on graphene electrodes

Y. Gao,[1] Y. S. Zhou,[1] W. Xiong,[1] L. J. Jiang,[1] M. Mahjouri-samani,[1] P. Thirugnanam,[1] X. Huang,[1] M. M. Wang,[1,2] L. Jiang,[2] and Y. F. Lu[1,a]
[1]*Department of Electrical Engineering, University of Nebraska-Lincoln, Lincoln, Nebraska 68588-0511, USA*
[2]*Department of Mechanical and Automation Engineering, Beijing Institute of Technology, 100081 Beijing, People's Republic of China*

(Received 18 February 2013; accepted 18 March 2013; published online 7 June 2013)

In this study, graphene-based supercapacitors with optical transparency and mechanical flexibility have been achieved using a combination of poly(vinyl alcohol)/phosphoric acid gel electrolyte and graphene electrodes. An optical transmittance of ∼67% in a wavelength range of 500-800 nm and a 92.4% remnant capacitance under a bending angle of 80° have been achieved for the supercapacitors. The decrease in capacitance under bending is ascribed to the buckling of the graphene electrode in compression. The supercapacitors with high optical transparency, electrochemical stability, and mechanical flexibility hold promises for transparent and flexible electronics. [http://dx.doi.org/10.1063/1.4808242]

The ever-increasing portable electronics requires the optical transparency and mechanical flexibility in energy conversion and storage components.[1–4] As major energy storage devices, supercapacitors have been widely used in power electronics,[5–7] such as electric vehicles, digital communication instruments, and emergency doors on jet planes. In addition to power and energy densities, supercapacitors in portable electronics require optical transparency and mechanical flexibility.[8,9]

Supercapacitors store energy directly through the electrostatic charge accumulated at the electrode/electrolyte interfaces.[10] Carbon materials, including carbon nanotubes,[6] activated carbon,[5] carbon aerogels,[11] carbon nanofibers,[12] and templated porous carbon[13] have been extensively studied as supercapacitor electrodes because of their large specific surface area (SSA), high conductivity, lightweight, controllable pore size distribution, and chemical stability.[5] Graphene, a new carbon material having a single or few layer sp^2 carbon network, has been investigated as a new electrode material for energy storage due to its large electrical conductivity, high SSA along with facile manufacturing techniques.[14] Graphene also has exceptional optical transparency and mechanical strength, making it suitable for transparent and flexible electronics.[15–20] However, very few studies have been conducted to use graphene for optically transparent and mechanically flexible supercapacitors.[14,15] In addition, the electrochemical stability during mechanical deformation of supercapacitors has not been considered in the past.

In this study, transparent, flexible, and solid-state supercapacitors were fabricated using two graphene electrodes with poly(vinyl alcohol)/phosphoric acid (PVA/H_3PO_4) gel electrolyte. The gel electrolyte was used to replace the rigid packages and prevent electrolyte leakage. The optical, mechanical, and electrochemical performances of the supercapacitors have been confirmed in the research.

Graphene was formed on SiO_2/Si substrates by a rapid thermal process.[21] The fabrication process starts from preparing a clean SiO_2/Si substrate. First, a thin layer of amorphous carbon is deposited on the substrates, followed by a deposition of nickel (Ni) film using DC sputtering.

[a]Author to whom correspondence should be addressed. Electronic mail: ylu2@unl.edu. Tel.: (402) 472-8323. URL: http://lane.unl.edu.

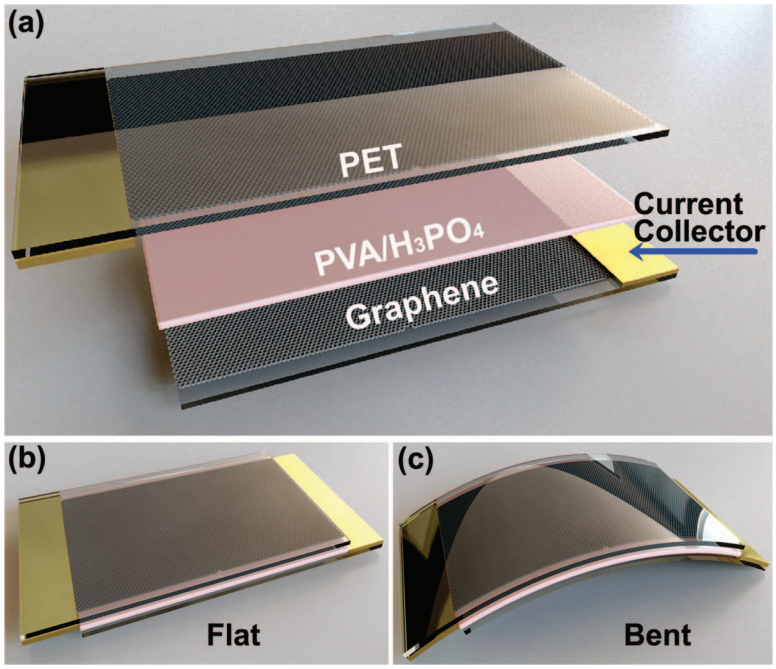

FIG. 1. (a) A schematic diagram of the supercapacitor when it is flat (b) and bent (c).

Typical thicknesses of the amorphous carbon and Ni films are 5 and 100 nm, respectively. Second, a rapid thermal annealing (RTA) process is conducted for the Ni/carbon/SiO_2/Si at 1000–1100 °C in a vacuum level around 20 mTorr (MTI, OTF-1200X-4-RTP). No gas precursor is required in the RTA process. The RTA process takes 1–2 min followed by a fast cooling process to room temperature. During the RTA process, the Ni top layer will be thermally evaporated once the graphene is formed. Large-area, uniform graphene sheets on SiO_2/Si substrate can be obtained by the end of RTA process.

The supercapacitors were fabricated using PVA/H_3PO_4 gel electrolytes sandwiched by two graphene electrodes. Graphene sheets were transferred onto polyethylene-terephthalate (PET, Dupont) substrates to form the electrodes. The PVA/H_3PO_4 gel electrolyte is prepared by mixing 1 g PVA powder with 10 ml deionized water and 0.8 g concentrated H_3PO_4.[1,14] Then, the PVA/H_3PO_4 gel electrolyte was spin-coated onto the graphene electrodes to serve as the ionic electrolyte and the separator.[1,14] Upon evaporation of excess water in the PVA/H_3PO_4 electrolyte, two graphene electrodes covered with the electrolyte were pressed against each other to form a transparent and flexible supercapacitor, as shown in Fig. 1.

A Renishaw inVia dispersive micro-Raman spectrometer with a 514 nm excitation source was used for Raman spectroscopic study. The transmittance spectra of the device were obtained by a UV-Visible spectrophotometer (Shimadzu, UV2401).

Electrochemical measurements of the devices were conducted on a CHI 760D (Shanghai, Chenhua, China) electrochemical workstation. The active graphene electrode contributed to form the electric double-layer has a size of 1 × 1 cm^2. The corresponding mass is ~1.596 × 10^{-7} g.

The capacitance of supercapacitors from a cyclic voltammogram was given by

$$C = \int i dV / S\nu\Delta V, \tag{1}$$

where i is the response current, ΔV is the potential range of cyclic voltammetry (CV), v is the potential scan rate, respectively. S is the area for the graphene electrodes.

The energy density of the supercapacitors was estimated by

$$E = C(\Delta U)^2 / 2, \tag{2}$$

where ΔU is the discharge potential after the iR drop.

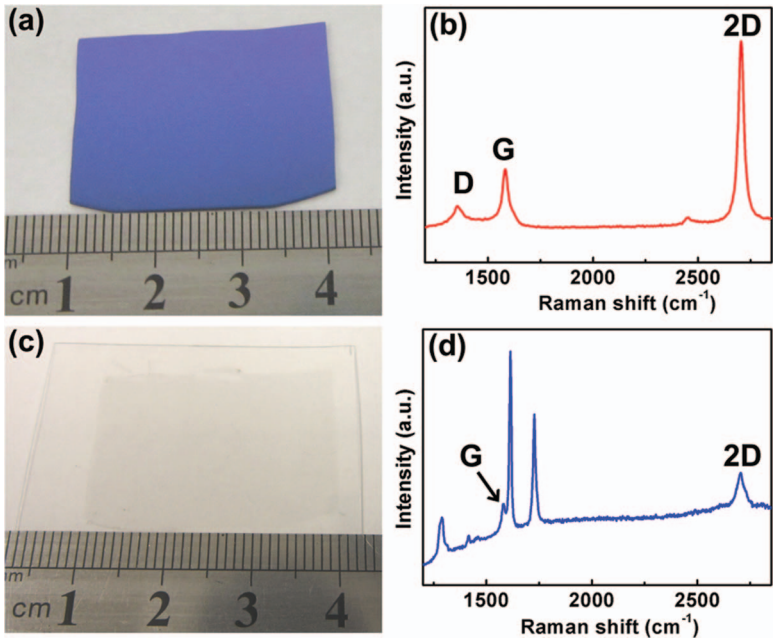

FIG. 2. (a) A photograph of a graphene film synthesized on a SiO_2/Si substrate. (b) The Raman spectrum of the graphene on the SiO_2/Si substrate. (c) The photograph of the graphene film transferred onto the PET substrate. (d) The Raman spectrum of the graphene on the PET substrate.

The power density of the supercapacitors was given by

$$P = E/t, \tag{3}$$

where t is the discharge time after the iR drop.

Figure 2(a) shows a typical photograph of a graphene film synthesized on a SiO_2/Si wafer with a size of 3×4 cm^2. The sheet resistance of the graphene is 100 Ω/□. The Raman spectrum confirms the growth of a monolayer graphene, as shown in Fig. 2(b). The weak D-band near 1350 cm^{-1} refers to the disorder in sp^2 carbon network.[22–25] A single Lorentzian profile of the 2D-band at ∼2700 cm^{-1} with a sharp line width of ∼30 cm^{-1} is observed, reflecting a high quality of the graphene layer.[22] Figure 2(c) shows a photograph of the optical transparent graphene film transferred onto a PET substrate. The Raman spectrum of the graphene on the PET substrate is shown in Fig. 2(d). In addition to the Raman peaks for the graphene (Fig. 2(b)), some Raman features of the PET substrate overlap with the graphene peaks.[23]

Figure 3(a) shows the photograph of the supercapacitor, which is transparent and flexible (Fig. 3(b)). Figure 3(c) shows the transmittance spectra of the graphene, the PET substrate, and the PVA/H_3PO_4 electrolyte with corresponding optical transmittances of ∼96%, ∼89%, and ∼87% in the wavelength range of 500–800 nm. At the same wavelength range, the optical transmittance of the supercapacitor reaches ∼67%, indicating a high optical transparency. The electrochemical properties of the supercapacitor in flat shape were studied by CV, as shown in Fig. 3(d). With increased scan rates up to 500 mV/s, the CV curves remain rectangular, indicating facile charging and discharging in the device. At 10 mV/s, the capacitance of the supercapacitor is 12.4 μF/cm^2.

The electrochemical performance of the supercapacitor was investigated under mechanical deformations. Figure 4(a) shows the remnant capacitance of the device at different bending angles. When the bending angle is less than 80°, the capacitance still maintains 92.4% of its original value. When the bending angle is further increased to 100°, the capacitance reduces below 90%.

The buckling (rippling) of the graphene electrode in compression is suggested as one reason causing the capacitance decrease under mechanical deformations. The capacitance of the

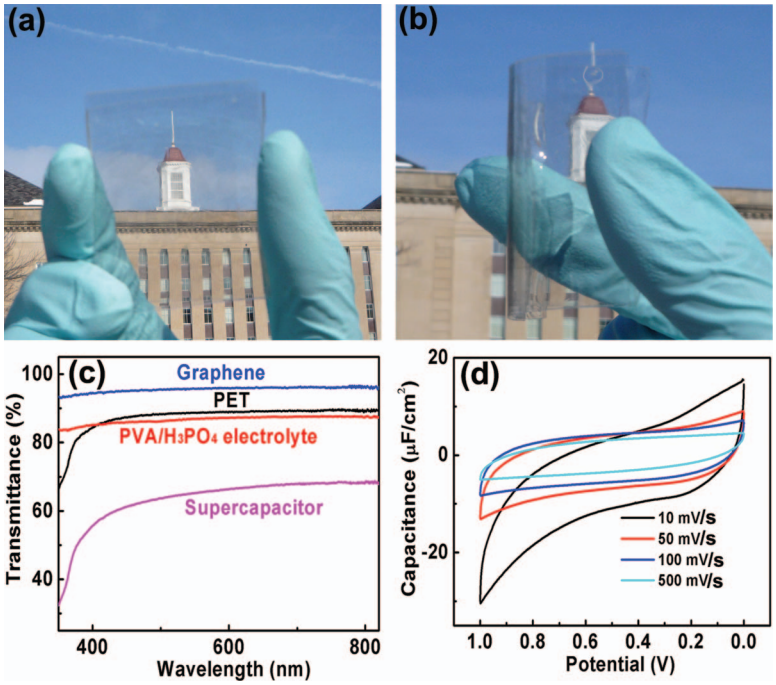

FIG. 3. (a) and (b) Photographs of the supercapacitor while flat and bent. (c) Transmittance spectra of the graphene, the PET substrate, and the electrolyte. (d) Electrochemical performance at different potential scan rates from 10 to 500 mV/s.

supercapacitor can be estimated using the following equation:[5]

$$1/C = 1/C_1 + 1/C_2, \tag{4}$$

where C_1 and C_2 are the capacitances of the electric double layers formed on both graphene electrodes. The capacitance of each electric double layer decreases with the thickness increase of the electric double layer, which can be approximately estimated using the following formula:[5]

$$C = \varepsilon_r \varepsilon_0 A/d, \tag{5}$$

where ε_r is the electrolyte dielectric constant, ε_0 is the permittivity of a vacuum, A is the specific surface area of the electrode accessible to the electrolyte ions, and d is the effective thickness of the electric double layer. When the supercapacitor is bent, both graphene electrodes are in tension and compression, respectively. The mechanical behavior of graphene demonstrates asymmetry in tensile versus compressive strain.[26] Galiotis *et al.*[26] reported that the graphene embedded in poly(methyl methacrylate) sustains up to 1.3% strain in tension but exibhits the buckling instability at 0.7% strain in compression. In another study, the buckling strains for graphene supported on substrates are 0.5%–0.6%.[27] In this study, the Raman shift of the 2D band was chosen to investigate the mechanical response to compressive strain in the graphene electrodes. The position of the 2D band as a function of the compressive strain is shown in Fig. 4(b). The inflection of the 2D band position at a compressive strain of 0.86% and the subsequent relaxation indicate that the graphene electrodes start to buckle at compressive strains around 0.86%. On the other hand, a tensile strain of 0.86% does not cause fracture and instability in the graphene electrodes.[27] Therefore, at bending angles (2θ) larger than 40° (strains > 0.86%), ripples are generated on the graphene electrodes in compression due to the weak van der Waals forces between the graphene and the PET substrate.[26] The ripples cause the increase in the thickness (d) of the electric double layer. Therefore, the capacitance of the compressed graphene electrode decreases, resulting into the decrease in the total capacitance of the supercapacitors.

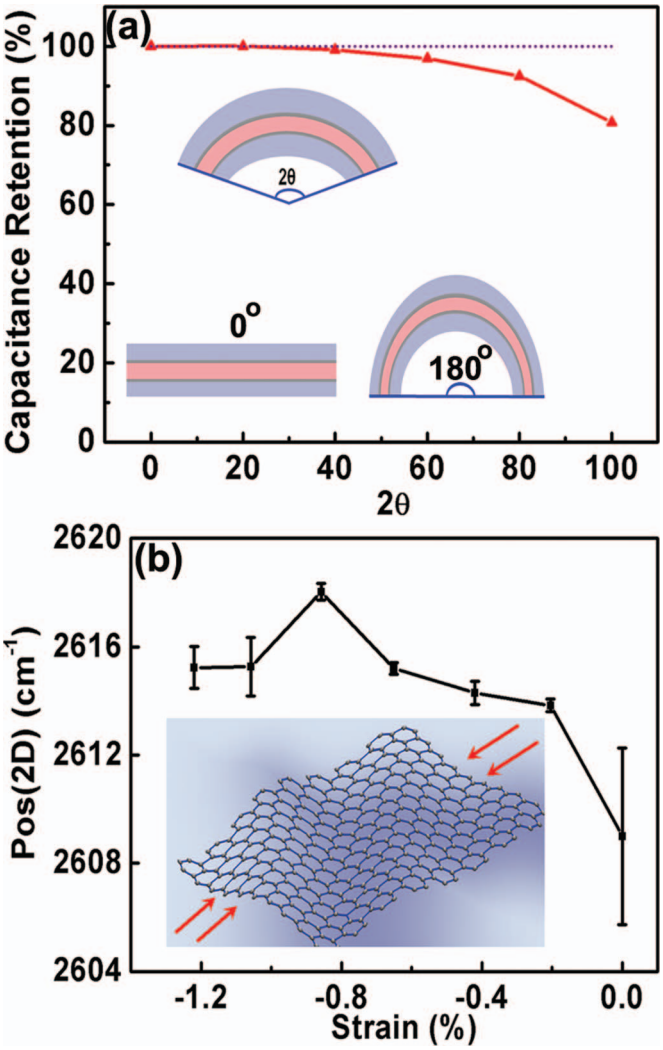

FIG. 4. (a) Remnant capacitance of the supercapacitors as a function of the bending angle. (b) Raman 2D peak position as a function of compressive strain in the graphene electrode.

The cyclic stability of the supercapacitors was also investigated under mechanical deformations, as shown in Fig. 5(a). A total of 1500 complete charge/discharge cycles were carried out at 0.38 μA/cm^2 to investigate the performance stability with and without bending ($2\theta = 80^\circ$). After 1500 cycles, approximately 96.4% of the initial capacitance was preserved for the supercapacitor without bending. While with a bending angle of 80°, approximately 93.6% of the initial capacitance was preserved. The energy and power densities for the supercapacitors with and without bending were calculated. Without bending, the energy and power densities are 0.47 nWh/cm^2 (2.94 Wh/kg) and 70 μW/cm^2 (438.6 kW/kg), respectively, as shown in Fig. 5(b). Compared to the studies reported previously using graphene electrodes,[15,28–32] the supercapacitor demonstrates lower energy density, which is ascribed to the confliction in achieving high transparency and high energy density at the same time.[32,33] With the bending angle of 80°, the remnant energy and power densities are 0.43 nWh/cm^2 (92.3%) and 62.7 μW/cm^2 (89.6%), respectively. These results demonstrate the electrochemical stability of the supercapacitors under mechanical deformations.

In summary, transparent, flexible, and solid-state graphene-based supercapacitors have been developed. An optical transmittance of ~67% in the wavelength range of 500–800 nm has been achieved for the supercapacitors. The electrochemical performance of the device is systematically

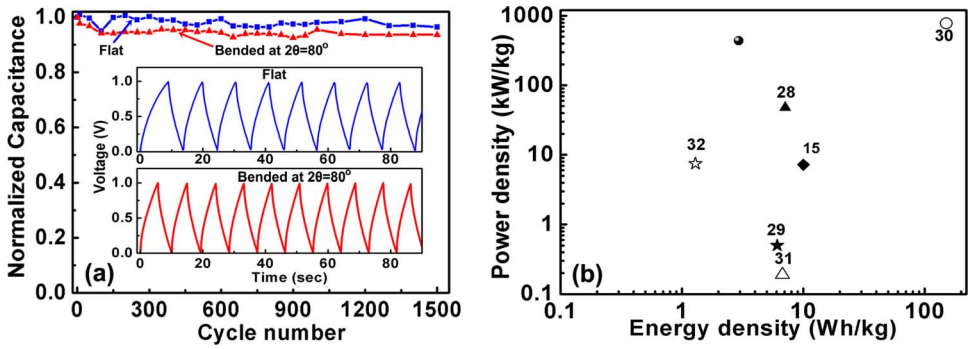

FIG. 5. (a) The 1500 charge-discharge cycles at a constant current density of 0.38 μA/cm^2. (b) Ragone plot for the transparent and flexible supercapacitor using graphene electrodes (solid circle), compared with the values from Refs. 15, 28–32.

evaluated under mechanical deformations. A 92.4% remnant capacitance at a bending angle of 80° has been achieved for the supercapacitors. The decrease in capacitance under bending is ascribed to the buckling of the graphene electrode in compression. After bending at 80° for 1500 cycles, only a small decrease in capacitance was observed, indicating its high electrochemical stability.

This research work was financially supported by the National Science Foundation (Grant Nos. CMMI 0852729, CMMI 0900419, and CMMI 1129613), Nebraska Center for Energy Science Research, and Office of Naval Research (Grant No. N00014-09-1-0943).

[1] S. Ju, J. Li, J. Liu, P. C. Chen, Y. G. Ha, F. Ishikawa, H. Chang, C. Zhou, A. Facchetti, D. B. Janes, and T. J. Marks, Nano Lett. **8**, 997 (2008).
[2] S. Ju, A. Facchetti, X. Xuan, J. Liu, F. Ishikawa, P. D. Ye, C. Zhou, T. J. Marks, and D. B. Janes, Nat. Nanotechnol. **2**, 378 (2007).
[3] M. Kaempgen, C. K. Chan, J. Ma, Y. Cui, and G. Gruner, Nano Lett. **9**, 1872 (2009).
[4] D. Wei, S. J. Wakeham, T. W. Ng, M. J. Thwaites, H. Brown, and P. Beecher, Electrochem. Commun. **11**, 2285 (2009).
[5] L. L. Zhang and X. S. Zhao, Chem. Soc. Rev. **38**, 2520 (2009).
[6] K. H. An, W. S. Kim, Y. S. Park, Y. C. Choi, S. M. Lee, D. C. Chung, D. J. Bae, S. C. Y. Lim, and H. Lee, Adv. Mater. **13**, 497 (2001).
[7] A. Izadi-Najafabadi, T. Yamada, D. N. Futaba, M. Yudasaka, H. Takagi, H. Hatori, S. Iijima, and K. Hata, ACS Nano **5**, 811 (2011).
[8] Y. Hu, H. Zhu, J. Wang, and Z. Chen, J. Alloys Compd. **509**, 10234 (2011).
[9] G. R. Li, Z. P. Feng, Y. N. Ou, D. Wu, R. W. Fu, and Y. X. Tong, Langmuir **26**, 2209 (2010).
[10] A. Burke, J. Power Sources **91**, 37 (2000).
[11] U. Fischer, R. Saliger, V. Bock, R. Petricevic, and J. Fricke, J. Porous Mater. **4**, 281 (1997).
[12] S. H. Yoon, S. Lim, Y. Song, Y. Ota, W. Qiao, A. Tanaka, and I. Mochida, Carbon **42**, 1723 (2004).
[13] R. Ryoo, S. H. Joo, and S. Jun, J. Phys. Chem. B **103**, 7743 (1999).
[14] J. J. Yoo, K. Balakrishnan, J. Huang, V. Meunier, B. G. Sumpter, A. Srivastava, M. Conway, A. L. M. Reddy, J. Yu, R. Vajtai, and P. M. Ajayan, Nano Lett. **11**, 1423 (2011).
[15] A. Yu, I. Roes, A. Davies, and Z. Chen, Appl. Phys. Lett. **96**, 253105 (2010).
[16] M. He, J. Jung, F. Qiu, and Z. Lin, J. Mater. Chem. **22**, 24254 (2012).
[17] T. H. Seo, J. P. Shim, S. J. Chae, G. Shin, B. K. Kim, D. S. Lee, Y. H. Lee, and E. K. Suh, Appl. Phys. Lett. **102**, 031116 (2013).
[18] J. Y. Lin, C. Y. Chan, and S. W. Chou, Chem. Commun. (Cambridge) **49**, 1440 (2013).
[19] J. Wang, X. Xin, and Z. Lin, Nanoscale **3**, 3040 (2011).
[20] J. H. Lee, K. Y. Lee, B. Kumar, N. T. Tien, N. E. Lee, and S. W. Kim, Energy Environ. Sci. **6**, 169 (2013).
[21] W. Xiong, Y. S. Zhou, L. J. Jiang, S. Amitabha, M. S. Masoud, Z. Q. Xie, Y. Gao, N. J. Ianno, L. Jiang, and Y. F. Lu, Adv. Mater. **25**, 630 (2013).
[22] A. Davies, P. Audette, B. Farrow, F. Hassan, Z. Chen, J. Y. Choi, and A. Yu, J. Phys. Chem. C **115**, 17612 (2011).
[23] T. Yu, Z. Ni, C. Du, Y. You, Y. Wang, and Z. Shen, J. Phys. Chem. C **112**, 12602 (2008).
[24] X. Li, Y. Zhu, W. Cai, M. Borysiak, B. Han, D. Chen, R. D. Piner, L. Colombo, and R. S. Ruoff, Nano Lett. **9**, 4359 (2009).
[25] A. C. Ferrari, J. C. Meyer, V. Scardaci, C. Casiraghi, M. Lazzeri, F. Mauri, S. Piscanec, D. Jiang, K. S. Novoselov, S. Roth, and A. K. Geim, Phys. Rev. Lett. **97**, 187401 (2006).
[26] G. Tsoukleri, J. Parthenios, K. Papagelis, I. Riaz, A. C. Ferrari, A. K. Geim, K. S. Novoselov, and C. Galiotis, Small **5**, 2397 (2009).
[27] A. Frank, G. Tsoukleri, J. Parthenios, K. Papagelis, I. Riaz, R. Jalil, K. S. Novoselov, and C. Galiotis, ACS Nano **4**, 3131 (2010).
[28] Z. Xu, Z. Li, C. M. B. Holt, X. Tan, H. Wang, B. S. Amirkhiz, T. Stephenson, and D. Mitlin, J. Phys. Chem. Lett. **3**, 2928 (2012).

[29] D. Sun, X. Yan, J. Lang, and Q. Xue, J. Power Sources **222**, 52 (2013).
[30] X. Yang, J. Zhu, L. Qiu, and D. Li, Adv. Mater. **23**, 2833 (2011).
[31] L. T. Le, M. H. Ervin, H. Qiu, B. E. Fuchs, and W. Y. Lee, Electrochem. Commun. **13**, 355 (2011).
[32] P. C. Chen, G. Shen, S. Sukcharoenchoke, and C. Zhou, Appl. Phys. Lett. **94**, 043113 (2009).
[33] Y. Yang, S. Jeong, L. Hu, H. Wu, S. W. Lee, and Y. Cui, Proc. Natl. Acad. Sci. U.S.A. **108**, 13013–13018 (2011).